EUROPEAN ORGANIZATION FOR NUCLEAR RESEARCH

CERN-PPE/92-114
5 June 1992

PROTON-ANTIPROTON ANNIHILATION INTO $\eta\eta\pi$ -- OBSERVATION OF A SCALAR RESONANCE DECAYING INTO $\eta\eta$

The Crystal Barrel Collaboration

C. Amsler[13], I. Augustin[6,a], C.A. Baker[11], B.M. Barnett[9,13], C.J. Batty[11], R. Beckmann[5], K. Beuchert[2], P. Birien[1], J. Bistirlich[1], P. Blüm[6], R. Bossingham[1],H. Bossy[1], K. Braune[10], D.V. Bugg[7], M. Burchell[4], T. Case[1], A. Cooper[7], K.M. Crowe[1], H.P. Dietz[10], S. von Dombrowski[13], M. Doser[4], W. Dünnweber[10], D. Engelhardt[6], M. Englert[10], M.A. Faessler[10], C. Felix[10], G. Folger[10], R. Hackmann[9], R.P. Haddock[8], F.H. Heinsius[5], N.P. Hessey[4,11], P. Hidas[3], P. Illinger[10], D. Jamnik[10,b], Z. Jávorfi[3], H. Kalinowsky[9], B. Kämmle[5], T. Kiel[5], E. Klempt[9], H. Koch[2], K. Königsmann[10], C. Kolo[10], M. Kunze[2], R. Landua[4], J. Lüdemann[2,9], H. Matthaey[2], M. Merkel[9], J.P. Merlo[9], C.A. Meyer[13], U. Meyer-Berkhout[10], L. Montanet[4], A. Noble[13], K. Peters[9], G. Pinter[3], S. Ravndal[2],A.H. Sanjari[7], E. Schäfer[9], B. Schmid[1,13], P. Schmidt[5], S. Spanier[9], C. Straßburger[9], U. Strohbusch[5], M. Suffert[12], D. Urner[13], C. Völcker[10], D. Walther[2], U. Wiedner[5], N. Winter[6], J. Zoll[4], C. Zupancic[10]

ABSTRACT

The results of a measurement of $\bar{p}p$ annihilation at rest into $\eta\eta\pi^o$ are presented. An isoscalar $J^{PC} = 0^{++}$ resonance decaying into $\eta\eta$ is observed with a mass of 1560 ± 25 MeV/c^2 and a width of 245 ± 50 MeV/c^2.

---

1 University of California, LBL, Berkeley, CA 94720, USA.
2 Universität Bochum, D-4630 Bochum, Germany.
3 Academy of Science, H-1525 Budapest, Hungary.
4 CERN, CH-1211 Genève, Switzerland.
5 Universität Hamburg, D-2000 Hamburg, Germany.
6 Universität Karlsruhe, D-7500 Karlsruhe, Germany.
7 Queen Mary and Westfield College, London E1 4NS, UK.
8 University of California, Los Angeles, CA 90024, USA.
9 Universität Mainz, D-6500 Mainz, Germany.
10 Universität München, D-8000 München, Germany.
11 Rutherford Appleton Laboratory, Chilton, Didcot Ox11 0QX, UK.
12 Centre de Recherches Nucléaires, F-67037 Strasbourg, France.
13 Universität Zürich, Ch-8001 Zürich, Switzerland.
a) This letter is part of the Ph.D. thesis of I. Augustin, in preparation.
b) Permanent address: University of Ljubljana, Slovenia.

Baryon-antibaryon annihilations are often considered as a likely source of mesonic states enriched in glue, and even of gluonia, the hypothetical bound states of gluons predicted in several models of quantum chromodynamics. In the scalar meson sector, the $f_o(1590)$, with its peculiar decay pattern, is considered as one of the best gluonium candidates. It was discovered by the GAMS collaboration [1] in an investigation of the $\eta\eta$ system produced in charge exchange $\pi^- p$ and in central $\pi^- N$ interactions at high energy.

The Crystal Barrel Collaboration has undertaken a systematic study of proton-antiproton annihilations using an external 200 MeV/c antiproton beam from the CERN Low Energy Antiproton Ring (LEAR). We present in this letter the first results obtained on the reaction:

$$\bar{p}p \rightarrow \eta\eta\pi^o \rightarrow 6\gamma \qquad (1)$$

at rest and show that this reaction is dominated by the production of an $\eta\eta$ scalar resonance with mass and width compatible with those of the $f_o(1590)$. The antiprotons are stopped in a liquid hydrogen target placed at the centre of the Crystal Barrel detector. A detailed description of the detector will appear elsewhere [2]. Suffice it to say here that the Crystal Barrel is a magnetic detector which covers 98% of the full solid angle and is sensitive to both charged particles and photons. Charged particles coming from annihilations which have occurred in the vicinity of the centre of the detector are observed and measured in two proportional wire chambers (PWCs) and in a cylindrical jet drift chamber (JDC). Photons, produced in the decays $\pi^o \rightarrow 2\gamma$, $\eta \rightarrow 2\gamma$, $\omega \rightarrow \pi^o\gamma \rightarrow 3\gamma$, etc., are measured in an electromagnetic CsI calorimeter which surrounds the drift chamber.

As the results presented here depend primarily upon the performance of the electromagnetic calorimeter, we briefly describe its relevant characteristics. The calorimeter consists of 1380 CsI crystals, 16 radiation lengths thick, read out by photodiodes. It covers the polar angles between 12° and 168° and has complete coverage in azimuth. This gives a useable acceptance for shower measurement of 95% of 4π solid angle. The energy calibration of the crystals is achieved using the 2γ decay mode of the π^o, abundantly produced in $\bar{p}p$ annihilations, by requiring the standard mass for the reconstructed π^o. The energy resolution σ/E varies slightly from run to run, from 2.45% to 2.70% for 1 GeV photons for the data used in this work. The angular resolution is $\sigma = 20$ mrad in the polar and azimuthal angles for isolated high-energy showers.

The excellent beam conditions provided by LEAR, and the geometrical and kinematical selections applied to the data guarantee that nearly all the annihilations used in this experiment occur at rest in liquid hydrogen. This has important consequences for the analysis since the possible initial quantum states are then limited to S and P wave $\bar{p}p$ annihilation states.

The incident antiproton trigger is provided by a silicon beam counter placed just before the liquid hydrogen target. The trigger includes a veto against annihilations producing charged particles, using the on-line information provided by the PWC and the JDC. This permits an increase in the data acquisition rate for annihilations into neutral particles, which represent only 4% of all annihilations. We have accumulated in four run periods, 11.2×10^6 events corresponding to about 3×10^8 annihilations. This is the starting sample for the analysis of reaction (1). In a previous publication [3], we presented the results of an analysis of the reaction $\bar{p}p \rightarrow 3\pi^o \rightarrow 6\gamma$ based on ~ 10% of the present statistics. We now proceed with a brief description of the selection of reaction (1), following closely the method used in [3].

Of the raw data sample, we first reject 1.0×10^6 events with charged tracks which escaped on-line PWC and JDC detections. We then reject all events which do not correspond exactly to six well-identified electromagnetic (e.m.) showers with more than 20 MeV energy. This cut removes the bulk of the background (8.1×10^6 events) but also reduces the detection efficiency for the reaction of interest. This is because a fraction of the $\eta\eta\pi^o$ events does not lead to six

well-isolated e.m. showers of more than 20 MeV: showers may merge or photons may remain undetected and, conversely, one photon may manifest itself, by e.m. shower fluctuations, as two separated e.m. showers in the detectors. The overall efficiency for this selection will be discussed below. Of the remaining 2.1×10^6 events we require the approximate energy and momentum conservation conditions:

$$1700\,\text{MeV} < \sum_{i=1}^{6} E_i < 2050\,\text{MeV}$$

$$\left| \sum_{i=i}^{6} \vec{p}_i \right| < 100\,\text{MeV/c} \quad ,$$

where the index i runs over the six photon showers. We reject in this way 0.7×10^6 events and keep 1.38×10^6 events. To illustrate the quality of the data obtained at this level, we show in Fig. 1 the two photon invariant mass spectrum (15 combinations per event).

Kinematic fits are then applied to isolate reaction (1). A 4C fit (energy-momentum conservation) to $\bar{p}p \to 6\gamma$ yields 1.13×10^6 events with a confidence level (CL) larger than 1%, i.e. 82% of the total sample. Next, 7C fits imposing in addition the masses of the decaying π^o and η are applied to the surviving events to select reaction (1) and the reactions

$$\bar{p}p \to \pi^o\pi^o\pi^o \quad (2)$$
$$\bar{p}p \to \eta\pi^o\pi^o \quad (3)$$
$$\bar{p}p \to \eta\eta\eta \quad (4)$$
$$\bar{p}p \to \omega\omega \to 2\pi^o 2\gamma \to 6\gamma \quad (8C) \quad (5)$$
$$\bar{p}p \to \eta'\eta\pi^o \quad (6)$$
$$\bar{p}p \to \eta'\pi^o\pi^o \quad (7)$$

The three dominant processes are reaction (2) with 0.61×10^6 events at a confidence level CL > 1%, reaction (3) with 0.29×10^6 events at CL > 1%, and reaction (1) with 75.8×10^3 events at CL > 1%. The other channels represent less than 10%. The probability distributions for these 7C fits are flat above 10%, showing that the measurement errors on the kinematical variables are correct.

Note that there are 45 possible ways to combine six photons to form the final states (1) and (3), and 15 combinations to form (2): all these combinations were tested but, owing to the good resolution of the calorimeter, the combinatorial background turned out to be quite small. However, due to a partial kinematical overlap between the three dominant channels, the same event might yield a good 7C fit for more than one hypothesis; since our goal is to get a clean sample of $\eta\eta\pi^o$ events, and as the rate for this channel is small compared in particular to $3\pi^o$ or $\eta\pi^o\pi^o$, we ultimately keep a sample of 22492 events giving a 7C fit confidence level larger than 10% for reaction (1) and no fit with CL larger than 1% for any other hypothesis. We have estimated, by Monte Carlo simulation, that the background of non $\eta\eta\pi^o$ events in the final sample is less than 1%, and that the $\eta\eta\pi^o$ events which have been rejected have the same phase space distribution (i.e. on the $\eta\eta\pi^o$ Dalitz plot) as the events which are kept.

A global Monte Carlo simulation of the detector and of all the selections and cuts applied to the data show that the efficiency to reconstruct and identify reaction (1), including the 7C fit CL of 10%, is 29%, and that this efficiency is flat (within ±4%) over the full phase space. With this estimate of the global efficiency and a branching ratio of 38.9% for $\eta \to \gamma\gamma$, we find that reaction (1) represents about 0.2% of all annihilations.

Figure 2 shows the Dalitz plot of these 22492 events (two entries per event). The most conspicuous features of the plot are, on the one hand, the cross-like structure which may be attributed to the presence of $a_o(980) \to \eta\pi^o$ and, on the other hand, the accumulation of events which populate the band around an $\eta\eta$ invariant mass of 1550 MeV/c^2. To a lesser extent, one may also notice a second accumulation around an $\eta\eta$ invariant mass of 1440 MeV/c^2. The observation of two-body resonances ($\eta\pi$ and $\eta\eta$) in the final state, and in particular the fact that at least one of these resonances seem to correspond to the well established $a_o(980)$ meson, leads us to analyze the Dalitz plot in terms of $\eta\pi$ and $\eta\eta$ final state interactions (i.e. in terms of resonances only). An inclusion of a non-resonant $\pi\eta\eta$ amplitude does not yield a better description of the experimental Dalitz plot.

Since the final state has C = +1 and since only S and P states of $\bar{p}p$ have appreciable annihilation probabilities, the allowed initial states are limited to ^1S_o ($J^{PC} = 0^{-+}$), $^3P_1$ ($J^{PC} = 1^{++}$) and $^3P_2$ ($J^{PC} = 2^{++}$). The invariant transition amplitudes are constructed to satisfy total angular momentum and parity conservations, according to the method developed by Zemach [4]. The same method was applied in [3] to analyze reaction (2). The helicity formalism [5], also used in the final analysis of reaction (1), yields identical results.

Included in the transition amplitudes are relativistic Breit-Wigner propagators:

$$F(m) = W'_L(p)W'_\ell(q)\frac{m_0\Gamma_0}{m_0^2 - m^2 - im_0\Gamma(m)}$$

with

$$\Gamma(m) = \Gamma_0\frac{m_0}{m}\frac{q}{q_0}\frac{W_\ell^2(q)}{W_\ell^2(q_0)} \quad .$$

Here, the nominal mass, width and decay momentum of the $\eta\pi$ (or $\eta\eta$) resonance are denoted by m_o, Γ_o and q_o; p is the momentum of the η (or π) recoiling against the $\eta\pi$ (or $\eta\eta$) system and L is the angular momentum between η and $\eta\pi$ (or between π and $\eta\eta$) in the $\bar{p}p$ rest frame; q is the η momentum and ℓ the relative $\eta\pi$ (or $\eta\eta$) angular momentum in the $\eta\pi$ (or $\eta\eta$) rest frame . The quantities denoted by W are the Blatt-Weisskopf damping factors [7]. We have

$$W_o(q) = 1$$

$$W_1(q) = (q\rho)\left(\frac{2}{1+(q\rho)^2}\right)^{1/2}$$

$$W_2(q) = (q\rho)^2\left(\frac{13}{9+3(q\rho)^2+(q\rho)^4}\right)^{1/2},$$

with ρ = 1 fm. In the helicity formalism, $W'_\ell(q) = W_\ell(q)$ for any ℓ. When using Zemach's method $W'_\ell(q) = (q\rho)^{-\ell}\, W_\ell(q)$.

The interpretation of the $\eta\pi$ final state interaction requires the presence of the $a_o(980)$, (see Fig. 3a). We have attempted our own determination of the mass and width of the $a_o(980)$, using the regions of the Dalitz plot which are less affected by the reflection of possible $\eta\eta$ resonances, i.e. using the regions with $M^2(\eta_1\pi) > 1.4$ GeV^2. Fitting a relativistic one-channel S-wave Breit-Wigner function $F_o[a_o(980)]$ to the $\eta_2\pi$ mass spectrum, we find:

$m_{a_0} = 982 \pm 2$ MeV/c^2

$\Gamma_{a_0} = 54 \pm 10$ MeV/c^2 ,

in excellent agreement with the Particle Data Group values [6]: m = 983.3 ± 2.6 MeV/c^2, and Γ = 57 ± 11 MeV/c^2. The errors were estimated by trying several forms of background and fitting regions. In the following, we shall use our values to represent the $a_o(980)$.

The other $\eta\pi$ known resonance which could be present in the Dalitz plot is $a_2(1320)$: for completeness, we shall introduce it, using a D wave Breit-Wigner function F_2 [$a_2(1320)$], with m_{a_2} = 1334 MeV/c^2, and Γ_{a_2} = 113 MeV/c^2, the standard values for the $a_2(1320)$ observed in its $\eta\pi$ decay mode [6].

The interpretation of the $\eta\eta$ final state interaction is more involved. Let us first dispose of the $f_2(1270)$. It has been shown in [3] that the $f_2(1270) \rightarrow \pi^o\pi^o$ represents ~ 20% of the $3\pi^o$ annihilations. Using a ratio of branching ratios [6]

$$\frac{B\left[f_2(1270) \rightarrow \eta\eta \rightarrow 4\gamma\right]}{B\left[f_2(1270) \rightarrow \pi^0\pi^0 \rightarrow 4\gamma\right]} = 2.4 \times 10^{-3}$$

we would expect a contribution of less than 300 events to our $\eta\eta\pi$ sample, i.e. < 1.5%, an unmeasurable quantity: any attempt to introduce the $f_2(1270)$ in the fit confirms this conclusion.

The $\eta\eta$ enhancement at ~ 1400 MeV/c^2 (see Fig. 3b), is tentatively attributed to the $f_o(1400)$. The enhancement at ~ 1550 MeV/c^2, on the other hand, cannot be easily identified with any known single resonance. It may correspond to an overlap of several resonances: one of them could be the $f_2(1515)$ observed in reaction (2) [3]; this may decay into $\eta\eta$ and should therefore be introduced in this analysis. This is done, imposing the mass, width and quantum numbers observed in [3], i.e.:

$f_2(1515)$: m = 1515 MeV/c^2, Γ = 120 MeV/c^2 .

Note that $f_2(1515)$ is different from $f'_2(1525)$ whose main decay mode is $K\overline{K}$ [6]. The absence of $f'_2(1525)$ in $\bar{p}p \rightarrow K\overline{K}\,\pi^o$ [8] leads us to estimate that it could contribute at most 1% to reaction (1). However, $f_2(1515)$ differs from $f'_2(1525)$ only by a small difference in width and a non-measurable difference in mass. Under these conditions, the results of the fit will have to be treated as a possible mixed contribution of both states. With these masses and widths, neither $f_2(1515)$ nor $f'_2(1525)$ can explain the totality of the broad $\eta\eta$ enhancement observed at ~ 1550 MeV/c^2: we are therefore led to introduce another resonance, called temporarily $X_J(1550)$, with a central mass in the vicinity of 1550 MeV/c^2 and a width around 250 MeV/c^2. Nothing is known, *a priori*, on its spin. We shall first assume $J^{PC} = 0^{++}$ and check later that this assignment is unique.

The fitting method used is identical to the method applied in the analysis of our $3\pi^o$ annihilation data [3]. The Dalitz plot is divided into 854 cells, out of which 92 are traversed by the boundary of the Dalitz plot. By omitting the latter cells we reduce the total area by about 6%. Owing to the symmetry of the Dalitz plot we fit only the part below the first diagonal. The basic criterion to judge the quality of a fit is $\chi^2 = \Sigma_i\,(n_i - f_i)^2/n_i$, where n_i and f_i are the number of measured and predicted events in each cell, and the sum extends over all 381 cells.

For a given initial state (^1S_o, $^3P_1$, $^3P_2$), the relevant amplitudes are added coherently, so that the Dalitz plot density is compared to a function of the form:

$$
\begin{aligned}
I = \big| & \alpha_1 B_J [{}^1S_0, X_J(1550)] + \alpha_2 B_0 [{}^1S_0, f_0(1400)] \\
& + \alpha_3 B_2 [{}^1S_0, f_2(1515)] + \alpha_4 A_0 [{}^1S_0, a_0(980)] \\
& + \alpha_5 A_2 [{}^1S_0, a_2(1320)] \big|^2 \\
+ \big| & \beta_1 B_J [{}^3P_1, X_J(1550)] + \beta_2 B_0 [{}^3P_1, f_0(1400)] \\
& + \beta_3 B_2 [{}^3P_1, f_2(1515)] + \beta_4 A_0 [{}^3P_1, a_0(980)] \\
& + \beta_5 A_2 [{}^3P_1, a_2(1320)] \big|^2 \\
+ \big| & \gamma_1 B_2 [{}^3P_2, f_2(1515)] + \gamma_2 A_2 [{}^3P_2, a_2(1320)] \big|^2
\end{aligned}
\tag{8}
$$

where, for example, $B_J[{}^1S_o, X_J(1550)]$ is the amplitude for annihilation from the ${}^1S_o$ (0^{-+}) initial state, via the intermediate $\eta\eta$ resonance X_J with spin J at a mass of 1550 MeV/c^2. Analogously, the amplitudes involving $\eta\pi$ resonances are denoted by A_J. The complex parameters α_i (i = 1, 5), β_i (i = 1, 5) and γ_i (i = 1,2) are left free in the fit. The phases of α_1, β_1 and γ_1 are arbitrary and hence fixed at zero. For the initial states ${}^3P_1$ and ${}^3P_2$, the norm of, for example, $|A_J|^2$ is to be understood as a summation over the magnetic sub-states of the initial state. The transition amplitudes A_J and B_J are normalized so that the integration of each $|A_J|^2$ or $|B_J|^2$ over the Dalitz plot is equal to the total number of events. Each amplitude includes a Breit-Wigner propagator F(m) and is properly symmetrized with respect to the interchange of the two η mesons. For the reactions $\bar{p}p$ (${}^3P_1$ and ${}^3P_2$) $\rightarrow \pi^o f_2$ we restrict ourselves to the lowest possible angular momentum L = 1.

In a first attempt, we include all 12 amplitudes in the fit, assuming J = 0 for the $X_J(1550)$. This attempt (21 free parameters) yields a reasonable $\chi^2/N_{dof} = 1.12$, but several contributions turn out to be non-significant: in particular, the three $a_2(1320)$ amplitudes, as well as the ${}^3P_2$ contribution for $f_2(1515)/f'_2(1525)$.

We therefore repeat the fitting procedure, eliminating one by one the non-significant contributions and find that an equally good fit ($\chi^2/N_{dof} = 1.15$) can be achieved with only six amplitudes (10 free parameters): four contributions from ${}^1S_o$: $X_o(1550)$, $f_o(1400)$, $f_2(1515)/f'_2(1525)$ and $a_o(980)$, and two contributions from ${}^3P_1$: $X_o(1550)$ and $f_2(1515)/f'_2(1525)$. Moreover, no significant systematic deviations between the data and the fitted distributions can be detected on the Dalitz plot for this solution.

The fit has been repeated, using various values for the masses and widths of the $f_o(1400)$ and $X_o(1550)$; the optimum values are found to be:

$$m = 1430 \text{ MeV}/c^2, \quad \Gamma = 250 \text{ MeV}/c^2$$

and

$$m = 1560 \text{ MeV}/c^2, \quad \Gamma = 245 \text{ MeV}/c^2,$$

respectively. The fit is rather sensitive to the masses assigned to the two resonances, but is less sensitive to the widths. The errors we quote for the $X_o(1560)$ mass and the width (± 25 MeV/c^2 and ± 50 MeV/c^2) are mainly systematic and cover the spread of mass and width obtained for

this resonance when varying the fitting hypothesis. One of these hypotheses is to restrict ourselves to the ^1S_o initial state, allowing for all five amplitudes listed in (8): the fit is significantly worse than the best one, yielding a χ^2/N_{dof} of 1.84. The spin-parity assignment 2^{++} was also tried for the X(1560) resonance, repeating all the attempts made with J = 0. All these attempts were completely unsuccessful; the best χ^2/N_{dof} achieved with this spin hypothesis being χ^2/N_{dof} = 5.3, (see Fig. 4). We therefore conclude that we observe the production of a scalar resonance $f_o(1560)$, decaying into $\eta\eta$.

The results of the best fit are shown in Table 1. The errors are only statistical: they just come out from the minimization fitting procedure. We defer a detailed discussion of the actual uncertainties to a later publication. According to Table 1, 88% of reaction (1) originates from the ^1S_o $\bar{p}p$ initial state and large interference effects are observed between the four corresponding amplitudes. This explains the surprising features which may be observed in the Dalitz plot: one would naively expect that the decay-angle distributions of scalar resonances such as $a_o(980)$ and $f_o(1430)$ should be flat, that the maxima of the $f_o(1430)$ and $f_o(1560)$ to be at their fitted values, and that the intensity of the $a_o(980)$ should be about 7% as expected from the prominent peak in the mass projection, Fig. 3a.

The most striking result of the best fit is the large contribution of $f_o(1560)$ to $\bar{p}p$ annihilation into $\eta\eta\pi$: 43% from ^1S_o initial state and 6% from $^3P_1$. Comparing the ratio of the $f_2(1515)/f'_2(1525)$ production amplitudes from ^1S_o to $^3P_1$:

$$|\alpha_3/\beta_3| = 0.56 \pm 0.08 \quad (f_2 \to \eta\eta)$$

to the ratio observed for the $2\pi^o$ decay [3]:

$$|\alpha_3/\beta_3| = 0.78 \pm 0.10 \quad (f_2 \to \pi^o\pi^o),$$

one notes that these results are in fair agreement. However, the best fit rejects any $f_2(1515)/f'_2(1525)$ production from $^3P_2$. When this amplitude is left free in the fit, we get a non-significant contribution, so that the ratio from $^3P_2$ to $^3P_1$ satisfies the relation

$$|\gamma_1/\beta_3| < 0.03 \; (f_2 \to \eta\eta)$$

whereas this ratio was found to be 0.78 ± 0.19 for $f_2 \to 2\pi^o$ [3]. These results are, at first sight, inconsistent. However, if two states with the same J = 2 indeed coexist and mix in the mass region around 1520 MeV, the branching ratios for different final states may depend on the initial state [9]. Note also that the production of $f_2(1515)/f'_2(1525)$ remains marginal for annihilation into $\eta\eta\pi$ (~ 8%) and that alternative parametrizations of the annihilation probabilities (such as a coupled channel analysis) may lead to small amplitudes substantially different from ours.

The $\eta\eta\pi^o$ Dalitz plot obtained in the same experiment from a sample of $\bar{p}p$ annihilations into 10 photons, shows the same qualitative features as those observed with the six photon sample, confirming in particular the importance of $f_o(1560)$ production. This plot is not shown, it is indistinguishable from Fig. 2. These 10 photon events have been obtained by fitting first the 10 photon hypothesis (4C fit), then by selecting, with a 9C fit, the hypothesis:

$$\bar{p}p \to 4\pi^o\eta \;, \quad \eta \to 2\gamma$$

and finally, by reconstructing the decay $\eta \to 3\pi^o$ and keeping the events which give a good kinematic fit to the decay chain:

$$\bar{p}p \to \eta_1\eta_2\pi^o \;, \quad \eta_1 \to 3\pi^o \;, \quad \eta_2 \to 2\gamma \,.$$

The mass, width, quantum numbers and decay mode of the $f_o(1560)$ make it very similar to the $f_o(1590)$ discovered by GAMS [1]. The production and decay properties reported by GAMS and the fact that no place is left in the scalar meson nonet have made this state a strong candidate for the 0^{++} ground state glueball. Its production in $\bar{p}p$ annihilation (similar to central production) supports this candidacy. In addition, we note that the $2\pi^o$ decay mode, which is expected for a $q\bar{q}$ state, has not been observed, either in central production or in $\bar{p}p$ annihilation. To confirm the non $q\bar{q}$ nature of the $f_o(1560)$ requires studies of other final states such as $K\bar{K}$ and $\eta\eta'$. These studies are underway and should help clarify the suitability of the $f_o(1650)$ as a glueball candidate.

Acknowledgements

We would like to thank the technical staff of the LEAR machine group for their invaluable contributions to the success of the experiment. We acknowledge financial support from the German Bundesministerium für Forschung und Technologie, the Schweizerischer Nationalfonds, the British Science and Engineering Research Council and the U.S. Department of Energy (contract No. DE-FG03-87ER40323 and DE-AC03-76SF00098). K.K. acknowledges support from the Heisenberg Programme.

REFERENCES

[1] F. Binon, Nuovo Cimento 78A (1983) 313.
D. Alde et al., Phys. Lett. B201 (1988) 160.
[2] E. Aker et al., The Crystal Barrel Spectrometer at LEAR, Nucl. Instrum. Methods (accepted for publication).
[3] E. Aker et al., Phys. Lett. B 260 (1991) 249.
Table 1 in this reference contains a typographical error. The last line stating the symmetric traceless space tensor for the decay from the $^3P_2$ $\bar{p}p$ initial state should read: $S_{J,L\ell} = 1/2[\mathbf{q} \otimes (\mathbf{q} \times \mathbf{p}) + (\mathbf{q} \times \mathbf{p}) \otimes \mathbf{q})]$.
[4] Ch. Zemach, Phys. Rev. B140 (1965) 97, 109.
[5] M. Jacob and G.C. Wick, Annals of Phys. 7 (1959) 404.
C. Amsler and J.C. Bizot, Comp. Phys. Comm. 30 (1983) 21.
[6] Review of Particle Properties (PDG), Phys. Lett. 239 (1990) 1.
[7] J.M. Blatt and V. Weisskopf, Theoretical Nuclear Physics (Wiley, New York, 1952).
[8] B. Conforto et al., Nucl. Phys. B3 (1967) 469.
[9] J.F. Donoghue, Phys. Rev. D25 (1982) 1875.

Figure captions

Fig. 1 : a) The two photon invariant mass spectrum from the six photon event sample (15 combinations per event): one clearly sees the π^o and η peaks. b) Same two photon invariant mass spectrum of those pairs which do not contribute any of their two photons to the π^o mass window. The η signal becomes more apparent. The additional structures at around 960 MeV/c^2 and 780 MeV/c^2 are due to the η' and the ω, where in the latter case one low energy photon remained undetected.

Fig. 2 : Dalitz plot of the final sample of $\eta\eta\pi^o$ events used in the present analysis (two entries per event). The arrows and associated mass values indicate the prominent structures.

Fig. 3 : a) The $\eta\pi^o$ invariant mass spectrum. b) The $\eta\eta$ invariant mass spectrum. The histograms represent the final fit.

Fig. 4 : Distribution of the η polar angle with respect to the direction of the recoiling π^o in the $\eta\eta$ rest frame for events selected in the mass range 1530 MeV/c^2 < M($\eta\eta$) < 1590 MeV/c^2 (data points). This distribution is compared with the results of the best fit with J = 0 for $X_J(1560)$ (shaded histogram) and with J = 2 (bold line).

Table 1

Amplitudes and phases of best fit. The intensity ratios are determined with the requirement $\Sigma_i |\alpha_i|^2 + \Sigma_j |\beta_j|^2 = 1$.

Initial state	Intermediate state	Amplitudes and Phases $\alpha_i = \lvert\alpha_i\rvert e^{i\phi i}$ $\beta_i = \lvert\beta_i\rvert e^{i\theta i}$	Ratio (%)
^1S_o	$f_o(1560)\pi^o$	$\lvert\alpha_1\rvert = 0.659 \pm 0.019$ (stat)	43.4 ± 1.3
	$f_o(1430)\pi^o$	$\lvert\alpha_2\rvert = 0.640 \pm 0.027$	41.0 ± 1.8
	$f_2(1515)\pi^o$	$\lvert\alpha_3\rvert = 0.142 \pm 0.011$	2.0 ± 0.2
	$a_o(980)\eta$	$\lvert\alpha_4\rvert = 0.127 \pm 0.009$	1.6 ± 0.2
$^3P_1$	$f_o(1560)\pi^o$	$\lvert\beta_1\rvert = 0.236 \pm 0.070$	5.6 ± 1.7
	$f_2(1515)\pi^o$	$\lvert\beta_3\rvert = 0.253 \pm 0.031$	6.4 ± 0.8
		$\phi_{1,2} = 2.07 \pm 0.05$	
		$\phi_{1,3} = -1.78 \pm 0.08$	
		$\phi_{1,4} = 0.65 \pm 0.06$	
		$\theta_{1,3} = 0.23 \pm 0.25$	

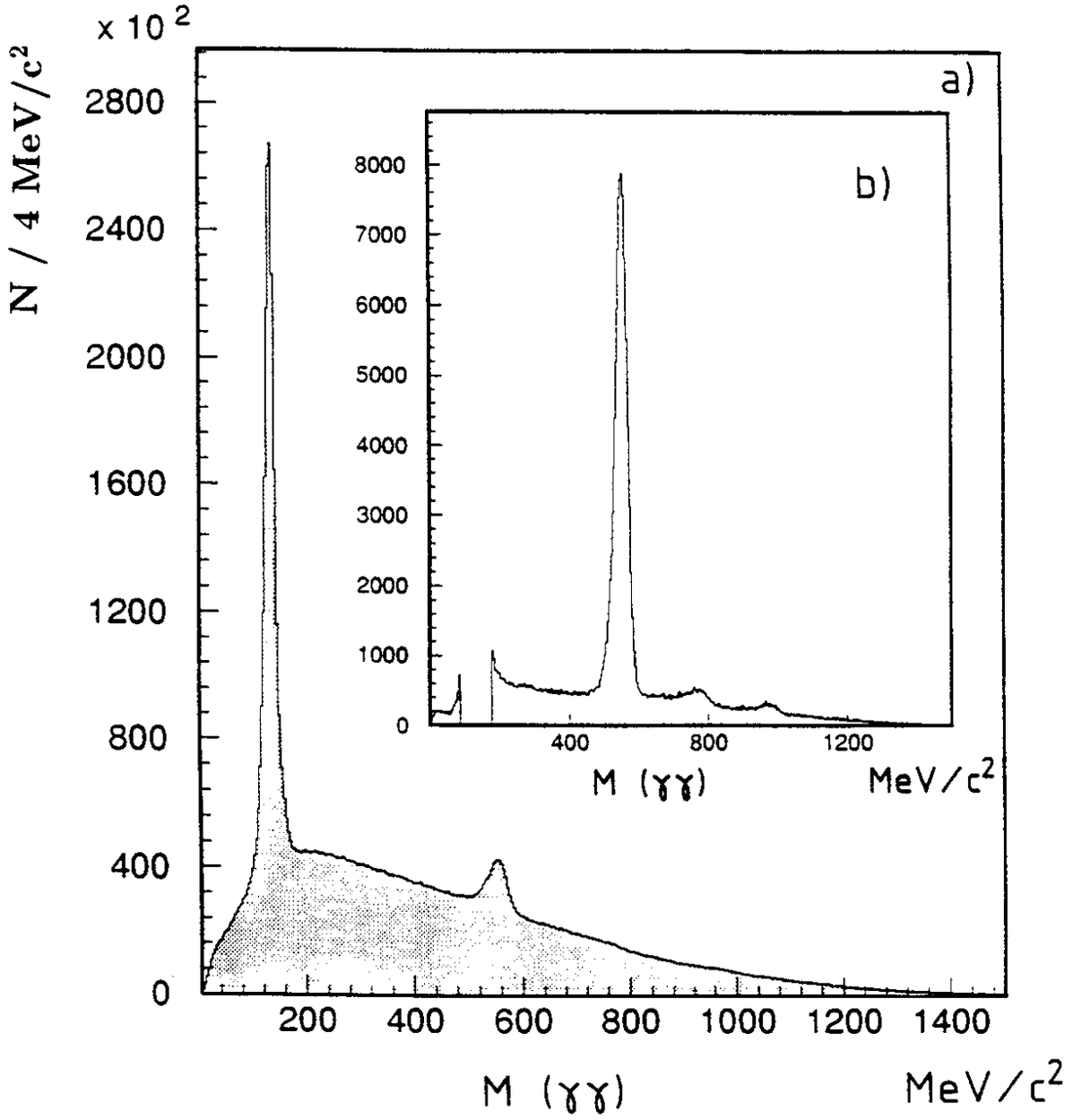
x 10 2
N / 4 MeV/c2
2800
2400
2000
1600
1200
800
400
0
200
400
600
800
1000
1200
1400
M (γγ)
MeV/c2
a)
b)
8000
7000
6000
5000
4000
3000
2000
1000
0
400
800
1200
M (γγ)
MeV/c2

Figure 1

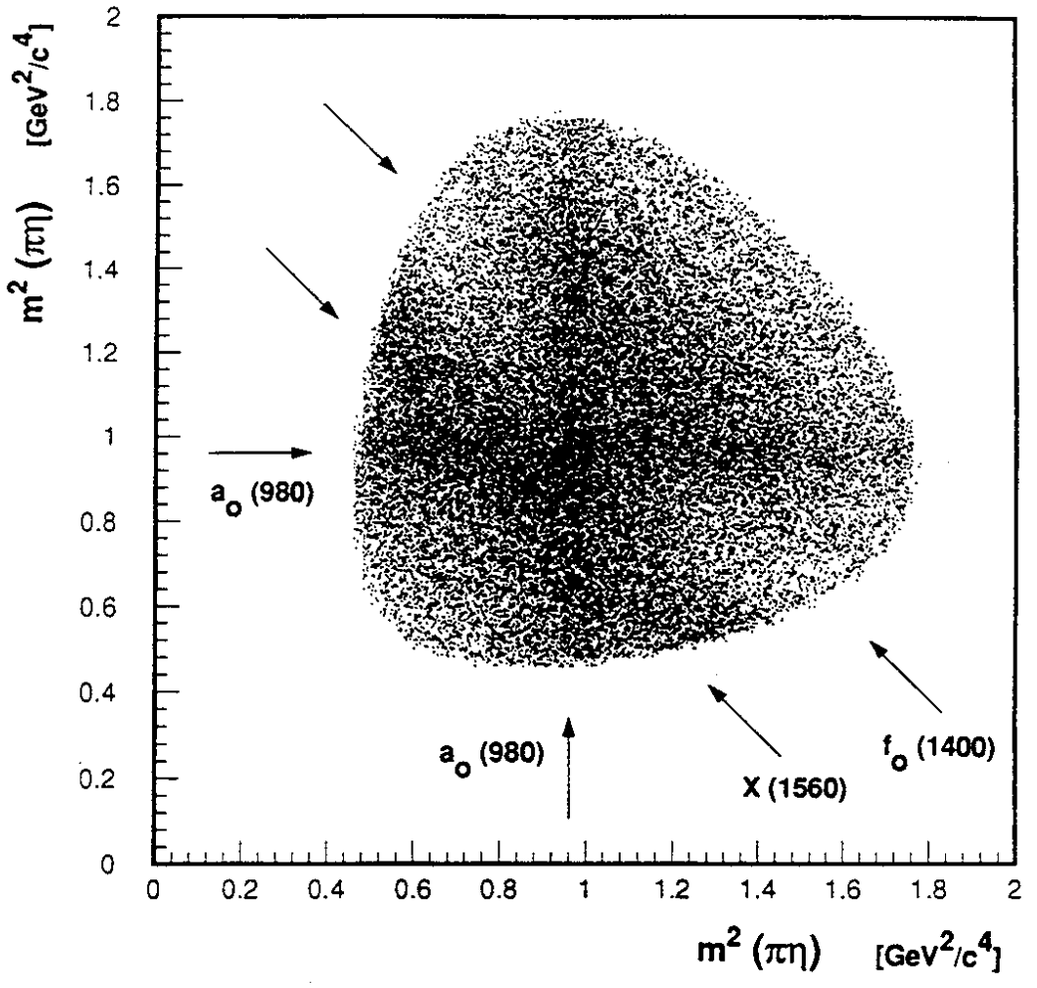

Figure 2

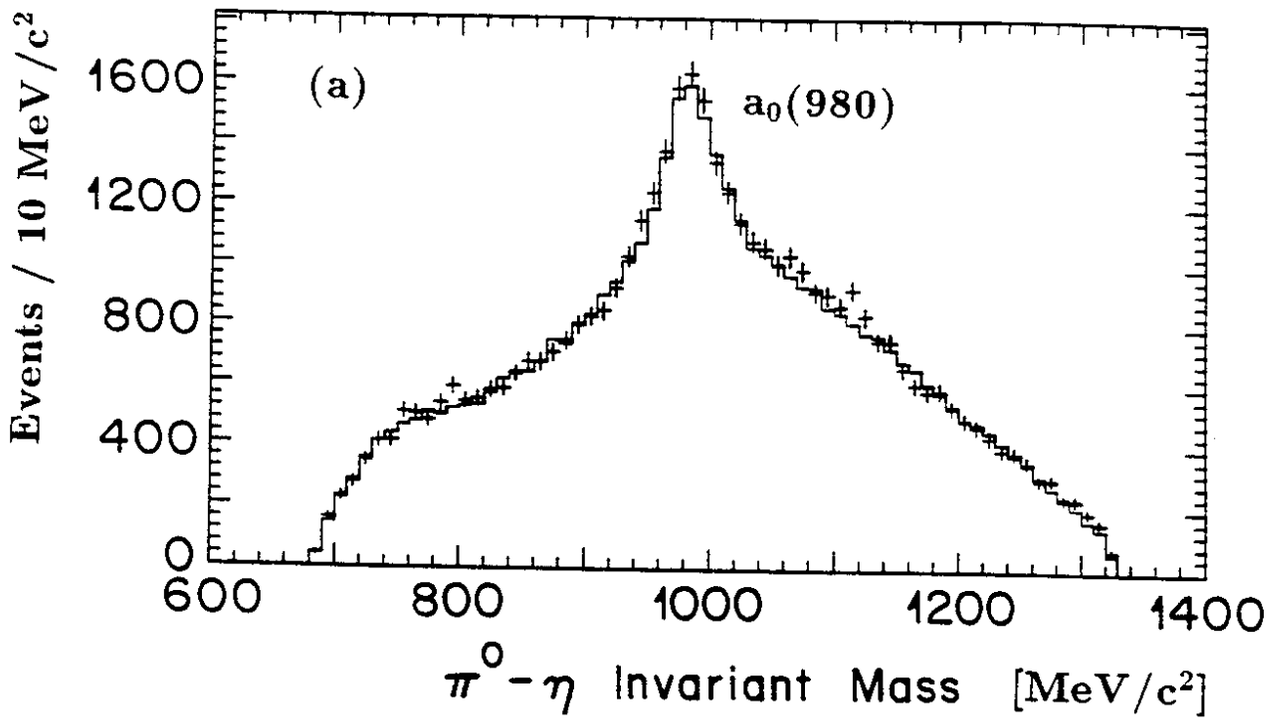
(a)
$a_0(980)$
Events / 10 MeV/c^2
1600
1200
800
400
0
600
800
1000
1200
1400
$\pi^0 - \eta$ Invariant Mass [MeV/c^2]

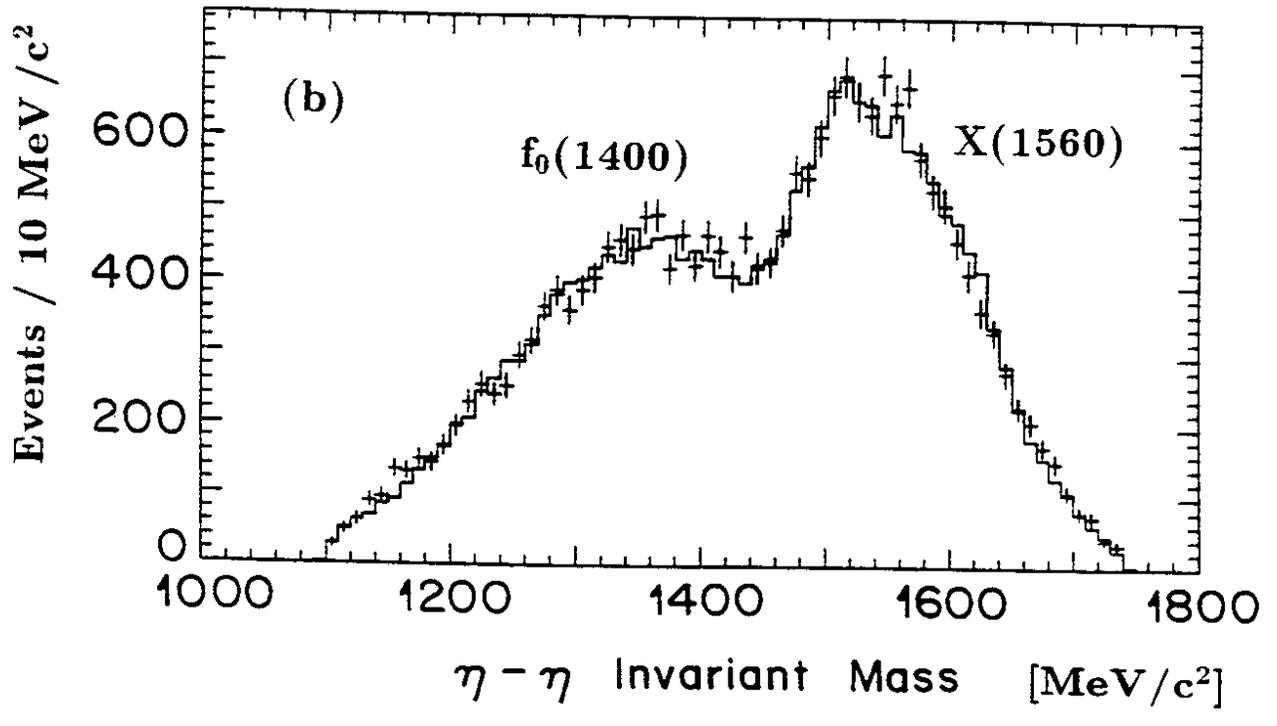
(b)
$f_0(1400)$
X(1560)
Events / 10 MeV/c^2
600
400
200
0
1000
1200
1400
1600
1800
$\eta - \eta$ Invariant Mass [MeV/c^2]

Figure 3

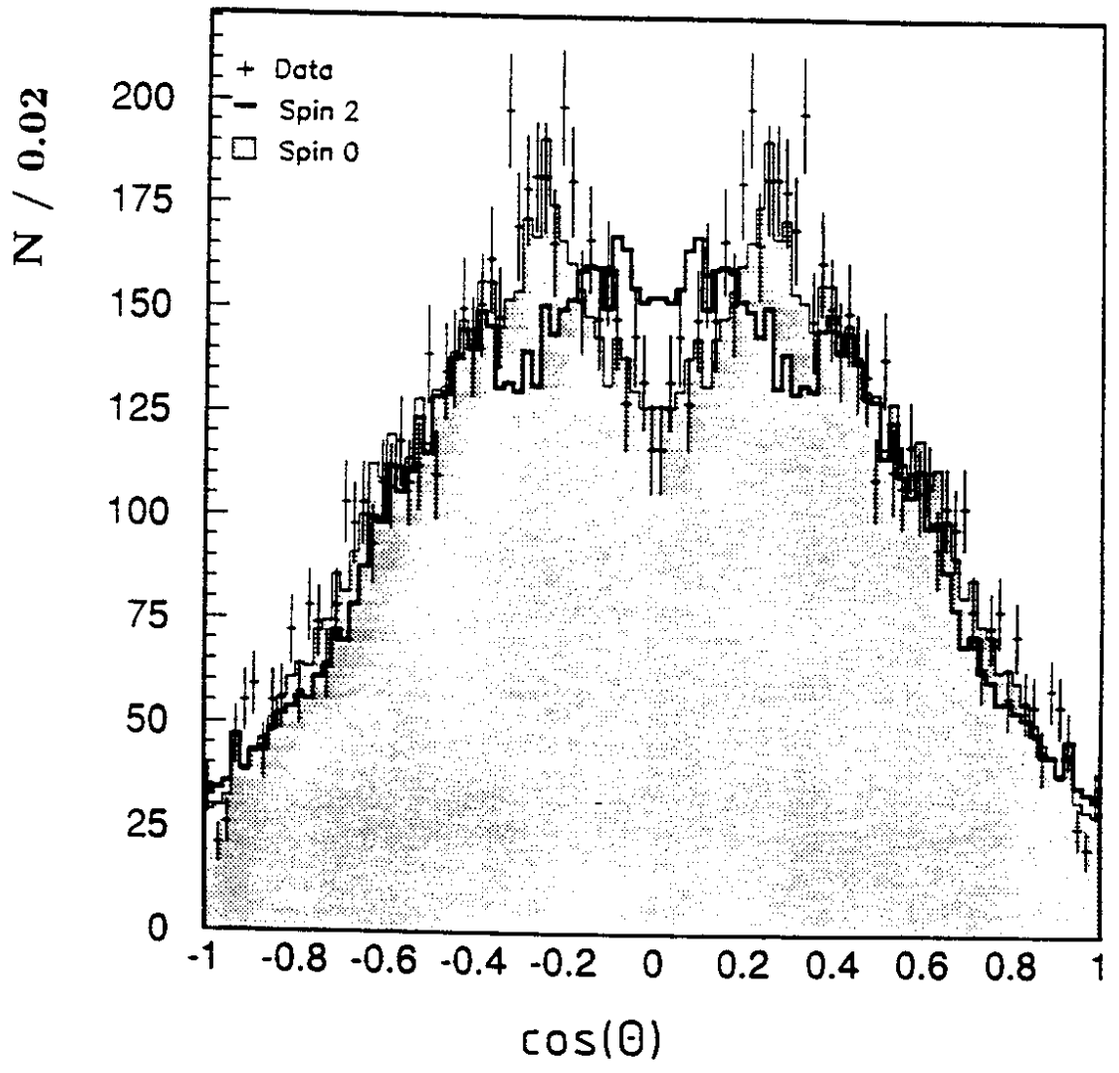
+ Data
Spin 2
Spin 0
N / 0.02
200
175
150
125
100
75
50
25
0
-1
-0.8
-0.6
-0.4
-0.2
0
0.2
0.4
0.6
0.8
1
cos(θ)

Figure 4